HHS Public Access

Author manuscript

Nat Genet. Author manuscript; available in PMC 2013 November 01.

Published in final edited form as:

Nat Genet. 2013 May ; 45(5): 531–536. doi:10.1038/ng.2590.

Recessive mutations in *DGKE* cause atypical hemolytic-uremic syndrome

Mathieu Lemaire[1,2,24], **Véronique Frémeaux-Bacchi**[3,4,24], **Franz Schaefer**[5,6], **Murim Choi**[1,2,7], **Wai Ho Tang**[8], **Moglie Le Quintrec**[4], **Fadi Fakhouri**[9], **Sophie Taque**[10], **François Nobili**[11], **Frank Martinez**[12], **Weizhen Ji**[1,2], **John D. Overton**[1,7], **Shrikant M. Mane**[1,7], **Gudrun Nürnberg**[13], **Janine Altmüller**[13], **Holger Thiele**[13], **Denis Morin**[14], **Georges Deschenes**[15], **Véronique Baudouin**[15], **Brigitte Llanas**[16], **Laure Collard**[17], **Mohammed A. Majid**[18], **Eva Simkova**[18], **Peter Nürnberg**[13,19,20], **Nathalie Rioux-Leclerc**[21], **Gilbert W. Moeckel**[22], **Marie Claire Gubler**[23], **John Hwa**[8], **Chantal Loirat**[15], and **Richard P. Lifton**[1,2,7]

[1]Department of Genetics, Yale University School of Medicine, New Haven, Connecticut, USA

[2]Howard Hughes Medical Institute, Yale University School of Medicine, New Haven, Connecticut, USA.

[3]Department of Immunology, Assistance Publique–Hôpitaux de Paris, Hôpital Européen Georges-Pompidou, Paris, France.

[4]UMRS 872, Centre de Recherche des Cordeliers, Paris, France.

[5]Division of Pediatric Nephrology and KFH Children's Kidney Center, Heidelberg University Medical Center, Heidelberg, Germany.

[6]Center for Pediatrics and Adolescent Medicine, Heidelberg University Medical Center, Heidelberg, Germany.

[7]Yale Center for Mendelian Genomics, Yale University School of Medicine, New Haven, Connecticut, USA.

[8]Department of Internal Medicine, Yale Cardiovascular Research Center, Section of Cardiovascular Medicine, Yale University School of Medicine, New Haven, Connecticut, USA.

Correspondence should be addressed to Véronique Frémeaux-Bacchi (veronique.fremeaux-bacchi@egp.aphp.fr) or Richard P Lifton(richard.lifton@yale.edu). .

[24]VFB and ML contributed equally to the work.

AUTHOR'S CONTRIBUTIONS: M.L., V.F.B., and R.P.L. designed experiments and analyzed data. M.C. and R.P.L. developed the exome analysis protocol. S.M.M., J.D.O., J.A. and H.T. directed the exome capture, DNA sequencing infrastructure and information technology. M.C., M.L., R.P.L., G.N. and P.N. performed bioinformatic and statistical analyses. M.L., W.J. and R.P.L. analyzed age of shared mutation. Sanger sequencing was done by M.L., W.J. and V.F.B.. W.H.T., J.H. and F. F. performed Western blotting experiments. M.L. performed the immunofluorescence studies. M.LQ. and F.F. performed the immunohistochemistry studies on human kidneys. F.Z., S.T., F.N., F.M., D.M., G.D., V.B., B.L., L.C., M.A.M., E.S. and C.L. ascertained and evaluated aHUS patients. C.L., V.F.B and F.S. recruited aHUS patients. N.R.L., G.W M., and M.C.G. provided renal pathology expertise. M.L., V.F.B. and R.P.L. wrote the manuscript.

COMPETING FINANCIAL INTERESTS F.S., F.F., C.L. and V.F.B. have received fees from Alexion Pharmaceuticals for invited lectures and are members of an expert board supported by Alexion Pharmaceuticals. C.L. is an unpaid coordinator for France for the clinical trial "Eculizumab in atypical HUS". P.N. is a founder, CEO, and shareholder of ATLAS Biolabs GmbH, a service provider for genomic analyses. The authors declare no other competing financial interests.

[9]Department of Nephrology, CHU Nantes, Nantes, France.

[10]Department of Pediatrics, CHU Rennes, Rennes, France.

[11]Department of Pediatrics, CHU Besançon, Besançon, France.

[12]Department of Nephrology, Assistance Publique–Hôpitaux de Paris, Hôpital Necker-Enfants Malades, Paris, France.

[13]Cologne Center for Genomics, University of Cologne, Cologne, Germany.

[14]Department of Pediatric Nephrology, CHU Montpellier, Montpellier, France.

[15]Department of Pediatric Nephrology, Assistance Publique–Hôpitaux de Paris, Hôpital universitaire Robert-Debré, Paris, France.

[16]Department of Pediatric Nephrology, CHU Bordeaux, Bordeaux, France.

[17]Department of Pediatrics, CHC Liège, Liège, Belgique.

[18]Department of Pediatrics, Pediatric Nephrology Unit, Dubai Hospital, Dubai, UAE.

[19]Center for Molecular Medicine Cologne, University of Cologne, Cologne, Germany.

[20]ATLAS Biolabs GmbH, Berlin, Germany.

[21]Department of Pathology, CHU Rennes, Rennes, France.

[22]Renal Pathology and Electron Microscopy Laboratory, Yale University School of Medicine, New Haven, Connecticut, USA.

[23]INSERM U983, Hôpital Necker-Enfants Malades, Paris, France.

Abstract

Pathologic thrombosis is a major cause of mortality. Hemolytic-uremic syndrome (HUS) features episodes of small vessel thrombosis resulting in microangiopathic hemolytic anemia, thrombocytopenia and renal failure[1]. Atypical HUS (aHUS) can result from genetic or autoimmune factors[2] that lead to pathologic complement cascade activation[3]. By exome sequencing we identify recessive mutations in *DGKE* (diacylglycerol kinase epsilon) that co-segregate with aHUS in 9 unrelated kindreds, defining a distinctive Mendelian disease. Affected patients present with aHUS before age 1, have persistent hypertension, hematuria and proteinuria (sometimes nephrotic range), and develop chronic kidney disease with age. DGKE is found in endothelium, platelets, and podocytes. Arachidonic acid-containing diacylglycerols (DAG) activate protein kinase C, which promotes thrombosis. DGKE normally inactivates DAG signaling. We infer that loss of *DGKE* function results in a pro-thrombotic state. These findings identify a new mechanism of pathologic thrombosis and kidney failure and have immediate implications for treatment of aHUS patients.

Mendelian forms of atypical HUS (aHUS) have implicated mutations in genes of the complement cascade, including complement factors B (*CFB*), H (*CFH*), and I (*CFI*), complement component 3 (*C3*), membrane cofactor protein (*MCP*) and thrombomodulin (*THBD*)[2]. All of these mutations result in unrestricted complement activation[3] Most are

transmitted as autosomal dominant traits with markedly reduced penetrance; only recessive mutations in *CFH* and *MCP* show apparently high penetrance[2]. Nonetheless, nearly half of aHUS patients without secondary causes have no discernable genetic or autoimmune abnormality[4].

We studied two unrelated families (kindreds 1 and 2), each with two siblings diagnosed with aHUS in infancy and unaffected unrelated parents. There were no pathogenic mutations in known aHUS genes nor anti-CFH antibodies (Supplementary Table 1). All four presented between 4 and 8 months of age with microangiopathic hemolytic anemia, thrombocytopenia and acute renal failure (Table 1 and Supplementary Table 2). Three had renal biopsies before age 3, all with pathology demonstrating chronic thrombotic microangiopathy (Table 1 and Fig. 1a-d). We performed exome sequencing of these 4 affected subjects (Supplementary Table 3). High quality variations from the reference sequence were called, their impact on encoded proteins determined and allele frequencies estimated.

We posited autosomal recessive transmission in these families and sought genes with rare homozygous or compound heterozygous variants (minor allele frequency < 1%, and homozygous/compound heterozygous genotypes not previously seen in databases) that were shared by both affected subjects (Supplementary Table 4). In kindred 1, there was a single novel homozygous variant shared by both affected subjects, and there was one novel shared compound heterozygous genotype in kindred 2. These novel genotypes occurred in the same gene, diacylglycerol kinase epsilon (*DGKE*). The former was a homozygous premature termination codon (p.Trp322*) while the latter genotype was a compound heterozygote for a frameshift (p.Val163Serfs*3) and a missense mutation (p.Arg63Pro); 3 unaffected siblings had zero or one of these variants (Fig. 2, Table 1 and Supplementary Fig. 1a).

To extend these findings, we sequenced *DGKE* in 47 additional unrelated probands with pediatric-onset aHUS and 36 adult-onset aHUS probands in whom mutation in known aHUS-associated genes or anti-CFH antibodies were not found (Supplementary Table 1). The results identified 6 additional index cases, harboring rare homozygous or compound heterozygous *DGKE* variants, all in pediatric-onset cases (Fig. 2, Table 1, and Supplementary Fig. 1a). Parental samples, available for all but one kindred, were heterozygous for one of the mutations with the exception of kindred 5, in which one mutation was apparently *de novo*. Additionally, kindred 9, independently ascertained in Germany with three affected subjects, showed complete linkage to the *DGKE* locus (LOD score 2.53; Supplementary Fig. 1b) and sequencing of all exons in the interval identified a homozygous *DGKE* p.Arg273Pro mutation (Fig. 2 and Supplementary Fig. 1a). These 9 patients all met clinical criteria for aHUS at presentation (Table 1 and Supplementary Table 2). Six had renal biopsies before age 2, all read as chronic thrombotic microangiopathy (Table 1 and Fig. 1e-g).

Collectively, the rare *DGKE* variants found in the 9 kindreds included 3 different premature termination codons, 2 frameshift mutations, 1 splice donor site mutation and two missense mutations that occur at conserved positions (Fig. 2 and Supplementary Fig. 1c). Only one of these variants, p.Trp322*, was previously seen among 8,475 subjects from NHLBI or Yale exome databases; this variant was heterozygous in two people of European ancestry.

p.Trp322* was found in five apparently unrelated aHUS subjects of European ancestry, and was homozygous in three. These three subjects shared an identical and extremely rare haplotype spanning no more than 400 kb at the *DGKE* locus (Supplementary Fig. 2 and Supplementary Table 5). This indicates a common ancestry for the mutation in each family, with the last common ancestor estimated to have occurred 53 generations ago (95% confidence interval, 33-73; Supplementary Fig. 3). The remote shared ancestry of the mutation is consistent with these 3 families not being closely related.

Twenty-two percent of siblings of index cases in these families (4/18) had aHUS, consistent with recessive transmission with high penetrance. Moreover, rare *DGKE* variants precisely cosegregate with aHUS in these families, yielding a LOD score of 8.9 (likelihood ratio of 7.9×10^8 in favor of linkage) for complete linkage of these variants to aHUS under a recessive model with rare phenocopies and high penetrance. Similarly, we found no homozygous/compound heterozygous damaging variants (premature termination, frameshift or splice site variants) among 8,475 subjects in NHLBI and Yale exome databases (Supplementary Fig. 4). The association of rare recessive genotypes with aHUS is extremely strong ($P = 2 \times 10^{-16}$, Fisher's exact test). Together, these genetic findings unequivocally establish recessive loss of function mutations in *DGKE* as the cause of aHUS in these families.

Patients with *DGKE* mutations all presented with aHUS in the first year of life (mean 0.5 years, range 0.3 – 0.9; Table 1). *DGKE* mutations were found in 9 of 22 pediatric aHUS patients with disease onset < 1 year of age, and 0 of 28 diagnosed after age 1 ($P = 2 \times 10^{-4}$). *DGKE* was a frequent cause of aHUS in the first year of life (13 of 49 aHUS cases, 27%) and accounted for 50% of familial disease in this age group (3 of 6 kindreds). This uniformly early age of onset defines a distinct subgroup of aHUS (Fig. 3a). The clinical course in *DGKE*-mutant subjects featured relapsing episodes of HUS before age 5 (Fig. 3b).

Abnormal complement activation is a feature of all previously described forms of aHUS[3]. Because *DGKE* encodes an intracellular enzyme, it is not obvious that complement activation plays a role in *DGKE*-mutant patients. Detailed assessment of the complement system revealed no compelling abnormality in any subject (Supplementary Table 1). Moreover, two patients with *DGKE* mutations had HUS relapses while on anti-complement therapy (eculizumab and fresh frozen plasma infusions, respectively) which are believed efficacious in patients with complement defects[5] (Supplementary Fig. 5 and Supplementary Table 2).

Among patients whose renal function recovered after the onset of aHUS, hypertension, microhematuria and proteinuria persisted in all but one (subject 5-3). In contrast, most patients with other aHUS subtypes have no residual renal abnormalities between episodes. Progression to chronic kidney disease (CKD) stages 4 and 5 was common by the second decade of life, long after the last acute episode of HUS (Fig. 3c). Interesingly, three patients developed nephrotic syndrome 3-5 years after disease onset, a very rare event in other forms of HUS. Repeat renal biopsies in these patients were read as chronic thrombotic microangiopathy (Supplementary Table 2). This is not likely a genotypic effect, because two

affected siblings have not developed nephrotic syndrome. Treating physicians did not report extra-renal phenotypes.

Three subjects received cadaveric renal transplantation at 2, 19 and 21 years using standard pre- and post-transplantation protocols (Supplementary Table 2). Two allografts have survived 2 and 4 years, while the other failed after 6 years due to chronic rejection. Importantly, there have been no HUS recurrences post-transplant. This contrasts with aHUS with defects in the soluble complement cascade in which recurrent HUS is very common and graft failure almost invariably occurs without anti-complement therapy[2].

DGKE was first cloned from a human endothelial cell line[6]; studies have noted high expression in testes and little expression elsewhere[6]. We examined DGKE expression by western blotting in human endothelial cells and platelets, the major cell types involved in thrombosis. We found DGKE expression in both (Fig. 4a-b). Moreover, staining of normal human kidney revealed DGKE in endothelium of glomerular capillaries and podocytes (Fig. 4c and Supplementary Fig. 7). Similar results were seen in rat, with colocalization with WT1, a podocyte marker (Supplementary Fig. 8). The specificity of this staining was established by parallel study of a renal biopsy of subject 2-7, a compound heterozygote for a frameshift mutation and a missense mutation in a beta-pleated sheet in the first *DGKE* C1 domain. Virtually no *DGKE* was seen in glomeruli of this patient (Fig. 4d and Supplementary Fig. 7a), while other antisera, such as anti-CD34, show normal staining (Supplementary Fig. 7c).

These findings establish recessive loss of function mutations in *DGKE* as a frequent cause of aHUS in the first year of life. Consanguinity, recurrence among siblings, persistence of hypertension, microhematuria and proteinuria (especially if in the nephrotic range) along with the absence of complement abnormalities, suggest the diagnosis of *DKGE* nephropathy. The molecular diagnosis of *DGKE* mutation should be straighforward.

DGKE is the first gene implicated in aHUS that is not an integral component of the complement cascade, raising the question of the pathophysiologic mechanism. *DGKE* preferentially phosphorylates arachidonic acid-containing diacylglycerol (AADAG) to the corresponding phosphatidic acid (PA)[7]. AADAG is a major signaling molecule of the diacylglycerol family, produced by hydrolysis of phosphatidylinositol 4,5-bisphosphate (PIP_2) by phospholipase C (PLC) in response to cell surface receptor signaling[8] (Supplementary Fig. 9). AADAGs activate protein kinase C (PKC)[9]. In endothelial cells, PKC increases production of various pro-thrombotic (von Willebrand factor[10], plasminogen activator inhibitor-1[11], platelet-activating factor[12], and tissue factor[13]) and antithrombotic factors such as tissue-type plasminogen activator[14] (Supplementary Fig. 10a). The factors determining the balance between these pro- and anti-thrombotic factors are poorly understood. AADAG-dependent PKC signaling also drives thrombin-induced platelet activation[15] (Supplementary Fig. 10b). Phosphorylation of AADAG to phosphatidic acid by DGKE terminates AADAG signaling. It is therefore plausible that loss of DGKE results in sustained AADAG signaling[16], resulting in a prothrombotic state. This mechanism is supported by experiments with R59022[17], a small molecule inhibitor of several DGK's

including DGKE. This produces platelet activation[18] and inhibition of endothelial prostacyclin production[19].

A similar mechanism may pertain to podocytes, where DAGs modifies slit diaphragm function[20], including inducing endocytosis of nephrin[21], an effect that could contribute to proteinuria and kidney failure. Additionally, VEGF signaling is essential for podocyte and renal endothelial cell survival, and loss of signaling in renal endothelium produces thrombotic microangiopathy[22,23]. Importantly, PKC-dependent downregulation of VEGFR2 has been reported in podocyte[24] and endothelial cells[25]. This interaction suggests a potential mechanism for the pronounced renal effects of this form of microangiopathy (Supplementary Fig. 10a). Further work will be required to determine the detailed biochemical mechanism(s) linking *DGKE* deficiency to aHUS.

The specific triggers that account for the episodic nature of acute attacks of aHUS are poorly understood. *Dgke*-null mice were not reported to have a thrombotic phenotype, perhaps because such an inciting factor was missing[26] or intrinsic species differences.

The universal findings of hypertension, microhematuria and proteinuria, and the unique finding of nephrotic syndrome among aHUS patients with *DGKE* mutations suggests they might play a role in other kidney diseases with similar glomerular phenotypes, such as systemic lupus erythematosis-associated glomerulonephritis[27], severe preeclampsia/HELLP syndrome[28], or membranoproliferative glomerulonephritis (MPGN)[29]. It is presently unclear whether the hypertension, microhematuria and proteinuria found in patients with *DGKE* mutations require prior acute episodes of HUS or whether it could occur in their absence.

In this regard, it is of great interest that during review of this manuscript a paper reporting 3 families with an early-onset MPGN-like syndrome featuring proteinuria and renal failure were described with recessive *DGKE* mutations. None of the affected patients were noted to have acute episodes suggesting aHUS, however histologic features of glomerular microangiopathy were noted. These authors also presented experimental evidence that loss of *DGKE* in podocytes might contribute to proteinuria and renal damage via aberrant activation of TRPC6[30].

Lastly, these findings have immediate implications for the treatment of aHUS. Current guidelines recommend that patients with aHUS be treated with eculizumab, an anti-C5 antibody that inhibits the complement cascade, or plasma therapy[5]. The absence of evidence linking *DGKE* deficiency to the complement cascade and relapses of acute HUS in these patients while receiving these therapies suggests they may not benefit *DGKE* patients. Moreover, unlike patients with soluble complement defects, it appears that renal transplantation can be efficacious and safe in patients with aHUS due to *DGKE* mutations, underscoring the importance of diagnosing *DGKE* nephropathy.

URLs. BLAST, http://blast.ncbi.nlm.nih.gov/Blast.cgi; ClustalW2, http://www.ebi.ac.uk/Tools/msa/clustalw2/; NCBI protein, http://www.ncbi.nlm.nih.gov/protein; NHLBI GO Exome Sequencing Project (ESP), https://esp.gs.washington.edu/drupal/; UCSC Genome browser, http://genome.ucsc.edu/; dbSNP, http://www.ncbi.nlm.nih.gov/snp.

METHODS

Methods and any associated references are available in the online version of the paper.

Accession codes

The *DGKE* variants described were deposited in dbSNP under batch accession number 1058996. mRNA and protein sequences are available at NCBI under the following accession numbers: human DGKE, NM_003647.2 and NP_003638.1, cow DGKE, NP_001179859.1, mouse Dgke, NP_062378.1, *Xenopus* dgke, NP_001087580.1, zebrafish dgke NP_001165699.1, fruitfly dgke, NP_725228.1, and worm dgk-2, NP_001024679.1. The reference protein sequences for pig (NP_001161117; 428 amino acids) and rat (NP_001034430; 407 amino acids) were ~70% shorter than expected. Full-length pig DGKE protein sequence (564 amino acids) was derived by translating the cDNA AK400222, while full-length rat DGKE protein (567 amino acids) was reassembled from the mRNA NM_001039341 by removing a short retained intron.

Detailed methods

aHUS kindreds

The French atypical HUS (aHUS) cohort[34] includes 139 patients from 131 unrelated kindreds with pediatric-onset aHUS and 36 unrelated subjects with adult-onset aHUS. These patients were recruited from 24 participating pediatric nephrology centers from France, and 1 from Belgium; 36 adult nephrology centers also enroll patients. This cohort includes 55 patients from 49 kindreds without mutation in any of the known aHUS genes or anti-CFH antibodies. One additional kindred including 3 affected subjects without mutations in known aHUS genes was ascertained in Dubai and Germany. IRB protocols were approved at all sites involved in the study and all subjects studied provided informed consent.

For all patients, relevant data were abstracted from detailed medical records. aHUS cases were defined using the classic diagnostic triad: microangiopathic hemolytic anemia (hemoglobin < 10 g/dL, with lactate dehydrogenase level > 250 IU/L, haptoglobin < 0.4 g/L or presence of schizocytes on blood smear), thrombocytopenia (platelets count lower than the lower limit of normal for age) and renal failure (serum creatinine level higher than the upper limit of normal for age). If one of the elements of the diagnostic triad was missing, clear evidence of thrombotic microangiopathic (TMA) lesions observed on a kidney biopsy was necessary to substantiate an aHUS diagnosis. Remission was defined by normalization of platelet and LDH levels, and relapse was defined by recurrence of microangiopathic hemolytic anemia, thrombocytopenia and/or a 25% increase in serum creatinine after at least two weeks remission. We specifically excluded patients with HUS caused by Shiga-toxin producing *Escherichia coli* and patients with secondary causes of HUS, such as drug exposure, autoimmune diseases, infections (*Streptococcus pneumoniae*, or human immunodeficiency virus), bone marrow or solid organ transplantation, and cobalamin deficiency.

Assessment of aHUS susceptibility factors (proteins and genes)

Assessment of complement system function was done at the complement laboratory at Hôpital Européen Georges-Pompidou (Paris, France), the National reference center for the evaluation of complement disorders. Blood samples from aHUS patients were collected for investigations of complement function and genetic analyses. Similar studies were performed in parallel on samples from 200 unrelated healthy French subjects to generate reference levels and validate any rare variants identified. Extensive investigations of the complement system were performed as described[35]. Briefly, the plasma concentrations of factors H and I (CFH, CFI) were measured by ELISA while levels of factors 3, 4 and B (C3, C4 and CFB) were measured by nephelometry. MCP surface expression was analyzed on granulocytes using anti-MCP phycoerythrin-conjugated antibodies (Serotec, UK). All patients were screened for anti-CFH antibodies and ADAMTS13 deficiency. All coding sequences of the *CFH*, *CFI*, *MCP, C3*, *CFB* and thrombomodulin (*THBD)* genes were sequenced as described[35]. Screening for unequal crossing over between homologous genes at the *CFH*, *CFHR1*, and *CFHR3* loci was done with multiplex ligation-dependent probe amplification (MLPA) from MRC Holland.

DNA sequencing and analysis

Genomic DNA from 2 aHUS index cases and 2 affected siblings was prepared and subjected to exome capture using NimbleGen 2.1M human exome capture arrays (Life technologies) followed by next generation sequencing on the Illumina sequencing platform as previously described[36]. Illumina's processing software ELAND (CASAVA 1.8.2) was used to map reads to the human reference genome (build 19), and SAMtools[37] was used to call single nucleotide variants and insertion/deletion at targeted bases. Variants with minor allele frequencies < 1% in the Yale (1,972 European subjects), NHLBI GO (4,300 European and 2,202 African American subjects; last accessed November, 2012), dbSNP (version 135) or 1000 Genomes (1,094 subjects of various ethnicities; May, 2011 data release) databases were selected and annotated for impact on the encoded protein and for conservation of the reference base and amino acid among orthologs across phylogeny. Variants of interest were verified by direct Sanger sequencing. Nomenclature of sequence *DGKE* variants is based on NCBI Reference Sequence NM_003647.

Genomic DNA of two affected members of kindred 9 underwent targeted enrichment of all exons from the interval 49.4-60.3 Mb on chromosome 17 based on evidence of linkage in this family (see below) followed by next generation sequencing. The targeted capture reagent was prepared by Roche NimbleGen (Madison, WI). Analysis prioritized homozygous protein-altering variants in the linked interval that were not present in the Ensembl SNP database, release 54.

To search for *DGKE* mutations in additional patients with aHUS the complete coding region of *DGKE* was amplified by PCR using specific oligonucleotide primer pairs for each of the 11 exons and subjected to direct Sanger sequencing. Samples from 48 index patients with aHUS but without mutation in the known aHUS genes and 38 index patients with heterozygous variants in known aHUS genes were sequenced.

DGKE variants were identified in exome data from subjects not known to have aHUS from Yale and NHLBI exome databases; potential compound heterozygous variants could only be identified in the Yale database since variants in NHLBI are not linked to genotypes.

Origin of *DGKE* p.Trp322*

Single nucleotide polymorphisms (SNP) flanking *DGKE* were selected using Haploview 4.2[38]. All had minor allele frequency > 10% and no violation of Hardy-Weinberg equilibrium ($p > 0.05$) among European subjects (CEU). SNPs were genotyped in 3 apparently unrelated subjects homozygous for p.Trp322* by PCR and direct Sanger sequencing. The boundaries of the homozygous segments were determined for each family by genotyping additional proximal and distal tag SNPs until heterozygous positions were recorded. This defined a shared homozygous haplotype comprising 16 SNPs no more than 400 kilobases in length.

The population frequency of the shared haplotype was estimated from the frequency of the haplotype in each block of linkage disequilibrium (LD); a frequency of 0.1% was assigned to haplotypes not previously detected in HapMap CEU dataset.

Given the rarity of the haplotype bearing *DGKE* p.Trp322* in CEU subjects, we examined the ancestry of the siblings from kindred 1 who were homozygous for this mutation by principal component analysis (PCA). All tag SNP genotypes were extracted from exome sequence data using a Perl script that produces PLINK-compatible output files. These SNPs were combined with HapMap data (Phase II release, 2010-08-18). Tag SNPs extracted using PLINK's LD-based SNP pruning algorithm[39] were used as inputs to perform PCA with EIGENSTRAT software (version 3.0)[40].

DMLE+2.3 software was used to estimate the age of the most common ancestor carrying *DGKE* p.Trp322*[41]. DMLE+2.3 uses a Bayesian approach to infer mutation age of a given variant based on observed LD data from polymorphic markers located within the shared segment. Data for six polymorphic loci spanning the shared segment were entered as genotypes. To minimize bias from consanguinity, we treated the data from these 3 kindreds as 3 independent chromosomes; however, results were similar when data from 6 chromosomes were used. Results were also similar whether analyses were performed under a recessive or dominant genetic model. The three unrelated families harboring $DGKE^{W322*}$ are all from western European ancestry. We estimated western Europe's population growth rate (PGR) using census data from France with the equation $PGR = LN(T_1/T_0)/g$, where T_1 and T_0 are the French populations in the years 2009 (62.5M) and 1806 (21M), respectively, and g is the number of generations during this period (g = 8.1 assuming ~25 years per generation). With these parameters, PGR is estimated at 0.09. When using T_0 from the 1954 census data (42.8M; g = 2.2), PGR is 0.17. To calculate the proportion of sampled chromosomes (PSC), we used the following values: number of chromosomes for *DGKE* nephropathy patients harboring p.Trp322* (n = 8), estimated minor allele frequency in CEU subjects (MAF ≤0.01%, based on empiric data from control exomes), and Western Europe's population (P = 200 millions; PSC = n/[MAF×P×2 chromosomes]). A sensitivity analysis was performed with various combinations of PSC and PGR values centered around the estimates described above. The software ESTIAGE was used to ascertain whether results

obtained with DMLE+2.3 were plausible[42]. ESTIAGE uses a likelihood-based method to estimate mutation age from information related to polymorphic markers located within or at the boundaries of the shared homozygous segment. Twenty-four SNPs spanning the *DGKE* locus were used for input. Mutation rate was set to 2×10^{-8}. Examples of input files for both softwares are available upon request.

Analysis of linkage and association

Genome-wide analysis of linkage analysis in kindred 9 was performed by comparing inheritance of SNP genotypes (Affymetrix GeneChip® Human Mapping 250K SNP NspI Array) to the inheritance of aHUS in all pedigree members specifying aHUS as a rare recessive trait with high penetrance and rare phenocopies, as described. Multipoint LOD scores were calculated using ALLEGRO[43]. Haplotypes were reconstructed with ALLEGRO and presented graphically with HaploPainter[44].

The significance of rare *DGKE* variants in all aHUS kindreds was assessed by comparing their segregation to the inheritance of aHUS in the kindreds. Parametric LOD scores were calculated specifying aHUS in kindreds with *DGKE* mutations as an autosomal recessive trait with complete penetrance and zero phenocopies. Fisher's exact test was used to compare the prevalence of recessive *DGKE* variants among non-consanguineous index cases of pediatric-onset aHUS to the corresponding prevalence in 8,475 control exomes from NHLBI and Yale.

DGKE protein expression in platelets and endothelial cells

Venous blood was drawn from 3 healthy adult human volunteers and from 3 wild type C57/Bl6 adult mice at 8- and 18-weeks of age. Platelets were prepared from blood by differential centrifugation as described[45]. The cytoplasmic and membrane fractions of total protein extracts were harvested by subcellular protein fractionation (Thermo Scientific). Alternatively, whole platelet lysates were prepared by lysis with NP-40 in the presence of protease and phosphatase inhibitors. Whole cell protein extracts from human embryonic venous endothelial cells (HUVECs) were prepared in an analogous fashion.

For western blotting, 50 μg of cytoplasmic and membrane platelet extracts, and total platelet and endothelial protein extracts were subjected to SDS-PAGE and analysed by Western blotting. After blocking, the membranes were probed with the following primary antibodies: for mouse extracts, rabbit polyclonal anti-DGKE (1:1000; Abcam); for human extracts, mouse monoclonal anti-DGKE (1:1000; Sigma) or mouse monoclonal anti-DGKE (1:1000; R&D). Anti-β-tubulin (1:500; Santa Cruz) and anti-Na,K-ATPase (1:500; Cell Signaling) primary antibodies were also used as loading controls and to assess the purity of the cytoplasmic and membrane fractions, respectively. Secondary antibodies linked to horseradish peroxidase (1:5000; Thermo Scientific) and incubated with the membrane for 1 hour at room temperature.

Microscopy

We stained kidney sections from two adult subjects with peri-renal tumors and from aHUS patient 2-7. A standard DAB protocol for renal tissue was used for immunohistochemistry

using anti-DGKE and anti-CD34 antibodies. Briefly, paraffin was removed with xylene/alcohol and heat-induced antigen retrieval was done with 10mM citrate, pH 6.0. Endogenous peroxidase activity was quenched with hydrogen peroxide (H_2O_2). Slides were washed twice with TBS-Tween in between each of the following steps. After blocking with 5% human serum in TBS, the slides were incubated with primary antibodies for 1 h, biotin-labeled secondary antibody for 1 h, and then streptavidin-horseradish peroxidase (Dako, P0397) for 30 minutes. DAB reagent (Dako) was then applied for 5 or 30 minutes and slides were then washed in water. Hematoxylin counterstain was applied to slides before mounting. The primary antibodies included rabbit polyclonal anti-DGKE (1:50; Novus Biologicals) and mouse monoclonal anti-CD34 (1:50; DAKO). The immunoperoxidase protocol used for Supplementary Fig. 7d-e was similar except for the following modifications: the primary antibody was mouse monoclonal anti-DGKE (1:30; R&D) was applied overnight, at 4°C; Tris-EDTA pH9.0 was used for antigen retrieval; PBS-based blocking solution contained 4% bovine serum albumin, 10% normal goat serum, and 0.1% Triton X-100.

Kidney specimens were obtained from adult wild type rats following infusion of PBS and 4% paraformaldehyde and equilibration overnight in 30% sucrose solution prior to freezing. Cryostat sections were prepared from frozen tissue (thickness, 10 microns) and fixed using the Nakane protocol. Slides were washed three times with TBS in between each step described below. After permeabilization with 0.1% Triton X-100, slides were blocked with 10% goat serum, 1% bovine serum albumin and 0.1% Triton X-100 diluted in TBS at room temperature for 1 h. The slides were incubated with primary antibodies at 4°C overnight, and then with secondary antibodies for 1 h at room temperature. Slides were mounted with DAPI nuclear counterstain (Vector Laboratories). Primary antibodies used were directed against DGKE labeled secondary antibodies (Invitrogen) were used at 1:200.

Supplementary Material

Refer to Web version on PubMed Central for supplementary material.

ACKNOWLEDGEMENTS

We thank the aHUS subjects, their families, and the health care professionals whose participation made this study possible; Junhui Zhang, Carol Nelson-Williams, SueAnn Mentone, Delphine Beury and others members of the complement laboratory at Hôpital Européen Georges-Pompidou for technical support; the staff of the Yale Center for Genome Analysis for exome production; Shuta Ishibe, Shigeru Shibata, Ute Scholl, Marie-Agnes Dragon-Durey, Lubka Roumenina, Michal Malina, Quentin Vincent and Laurent Abel for helpful discussions; Diane Damotte for the anti-CD34 staining. This work was supported by NIH grants U54 HG006504 01 (Yale Center for Mendelian Genomics), P30 DK079310 05 (Yale O'Brien Center for Kidney Research) and UL1TR00142 07 (Yale Center for Translational Science Award), by grants from the Délégation Régionale à la Recherche Clinique, Assistance Publique – Hôpitaux de Paris to V.F.B., such as Programme Hospitalier de Recherche Clinique, (AOM08198), and the Association pour l'Information et la Recherche dans les maladies Rénales génétiques (AIRG France), and a grant from EURenOmics (2012-305608) to F.S. and V.F.B.. M.L. is the recipient of a Kidney Research Scientist Core Education and National Training (KRESCENT) Program Post-Doctoral Fellowship Award from the Kidney Foundation of Canada and is a member of the Investigative Medicine Ph.D. program at Yale University School of Medicine.

References

1. Neild GH. Haemolytic-uraemic syndrome in practice. Lancet. 1994; 343:398–401. [PubMed: 7905557]
2. Loirat C, Frémeaux-Bacchi V. Atypical hemolytic uremic syndrome. Orphanet J. Rare Dis. 2011; 6:60. [PubMed: 21902819]
3. Noris M, Mescia F, Remuzzi G. STEC-HUS, atypical HUS and TTP are all diseases of complement activation. Nat. Rev. Nephrol. 2012; 8:622–633. [PubMed: 22986360]
4. Noris M, Remuzzi G. Atypical hemolytic–uremic syndrome. N. Engl. J. Med. 2009; 361:1676–1687. [PubMed: 19846853]
5. Zuber J, Fakhouri F, Roumenina LT, Loirat C, Frémeaux-Bacchi V. Use of eculizumab for atypical haemolytic uraemic syndrome and C3 glomerulopathies. Nat. Rev. Nephrol. 2012; 8:643–657. [PubMed: 23026949]
6. Tang W, Bunting M, Zimmerman GA, McIntyre TM, Prescott SM. Molecular cloning of a novel human diacylglycerol kinase highly selective for arachidonate-containing substrates. J. Biol. Chem. 1996; 271:10237–10241. [PubMed: 8626589]
7. Shulga YV, Topham MK, Epand RM. Regulation and functions of diacylglycerol kinases. Chem. Rev. 2011; 111:6186–6208. [PubMed: 21800853]
8. Rhee SG. Regulation of phosphoinositide-specific phospholipase C. Annu. Rev. Biochem. 2001; 70:281–312. [PubMed: 11395409]
9. Pettitt TR, et al. Diacylglycerol and phosphatidate generated by phospholipases C and D, respectively, have distinct fatty acid compositions and functions. Phospholipase D-derived diacylglycerol does not activate protein kinase C in porcine aortic endothelial cells. J. Biol. Chem. 1997; 272:17354–17359. [PubMed: 9211874]
10. Carew MA, Paleolog EM, Pearson JD. The roles of protein kinase C and intracellular Ca2+ in the secretion of von Willebrand factor from human vascular endothelial cells. Biochem. J. 1992; 286:631–635. [PubMed: 1530595]
11. Ren S, Shatadal S, Shen GX. Protein kinase C-beta mediates lipoprotein-induced generation of PAI-1 from vascular endothelial cells. Am. J. Physiol. Endocr. Metab. 2000; 278:E656–662.
12. Whatley RE, et al. The regulation of platelet-activating factor production in endothelial cells. The role of calcium and protein kinase C. J. Biol. Chem. 1989; 264:6325–6333. [PubMed: 2703492]
13. Herbert JM, Savi P, Laplace MC, Dumas A, Dol F. Chelerythrine, a selective protein kinase C inhibitor, counteracts pyrogen-induced expression of tissue factor without effect on thrombomodulin down-regulation in endothelial cells. Thromb. Res. 1993; 71:487–493. [PubMed: 8134908]
14. Levin EG, Marotti KR, Santell L. Protein kinase C and the stimulation of tissue plasminogen activator release from human endothelial cells. Dependence on the elevation of messenger RNA. J. Biol. Chem. 1989; 264:16030–16036. [PubMed: 2506174]
15. Offermans S. Activation of platelet function through G protein–coupled receptors. Circ. Res. 2006; 15:1293–1304.
16. Pettitt TR, Wakelam MJ. Diacylglycerol kinase epsilon, but not zeta, selectively removes polyunsaturated diacylglycerol, inducing altered protein kinase C distribution in vivo. J. Biol. Chem. 1999; 274:36181–36186. [PubMed: 10593903]
17. Yada Y, Ozeki T, Kanoh H, Nozawa Y. Purification and characterization of cytosolic diacylglycerol kinases of human platelets. J. Biol. Chem. 1990; 265:19237–19243. [PubMed: 2172248]
18. Nunn DL, Watson SP. A diacylglycerol kinase inhibitor, R59022, potentiates secretion by and aggregation of thrombin-stimulated human platelets. Biochem. J. 1987; 243:809–813. [PubMed: 2821994]
19. De Nucci G, Gryglewski RJ, Warner TD, Vane JR. Receptor-mediated release of endothelium-derived relaxing factor and prostacyclin from bovine aortic endothelial cells is coupled. Proc. Natl. Acad. Sci. U S A. 1988; 85:2334–2338. [PubMed: 2832851]
20. Hofmann T, et al. Direct activation of human TRPC6 and TRPC3 channels by diacylglycerol. Nature. 1999; 397:259–263. [PubMed: 9930701]

21. Quack I, et al. PKC mediates beta-arrestin2-dependent nephrin endocytosis in hyperglycemia. J. Biol. Chem. 2011; 286:12959–12970. [PubMed: 21321125]
22. Eremina V, et al. VEGF inhibition and renal thrombotic microangiopathy. N. Engl. J. Med. 2008; 358:1129–1136. [PubMed: 18337603]
23. Sison K, et al. Glomerular structure and function require paracrine, not autocrine, VEGF-VEGFR-2 signaling. J. Am. Soc. Nephrol. 2010; 21:1691–1701. [PubMed: 20688931]
24. Hoshi S, Nomoto K, Kuromitsu J, Tomari S, Nagata M. High glucose induced VEGF expression via PKC and ERK in glomerular podocytes. Biochem. Biophys. Res. Commun. 2002; 290:177–184. [PubMed: 11779150]
25. Rask-Madsen C, King GL. Differential regulation of VEGF signaling by PKC-alpha and PKC-epsilon in endothelial cells. Arterioscl. Throm. Vasc. 2008; 28:919–924.
26. Rodriguez de Turco EB, et al. Diacylglycerol kinase epsilon regulates seizure susceptibility and long-term potentiation through arachidonoyl-inositol lipid signaling. Proc. Natl. Acad. Sci. U S A. 2001; 98:4740–4745. [PubMed: 11287665]
27. Lansigan F, Isufi I, Tagoe CE. Microangiopathic haemolytic anaemia resembling thrombotic thrombocytopenic purpura in systemic lupus erythematosus: the role of ADAMTS13. Rheumatology. 2011; 50:824–829. [PubMed: 21149242]
28. Ganesan C, Maynard SE. Acute kidney injury in pregnancy: the thrombotic microangiopathies. J. Nephrol. 2011; 24:554–563. [PubMed: 21240869]
29. Skerka C, et al. Autoimmune forms of thrombotic micorangiopathy and membranoproliferative glomerulonephritis: Indications for a disease spectrum and common pathogenic principles. Mol. Immunol. 2009; 46:2801–2807. [PubMed: 19640589]
30. Ozaltin F, et al. DGKE variants cause a glomerular microangiopathy that mimics membranoproliferative GN. J. Am. Soc. Nephrol. 2012 doi: 10.1681/ASN.2012090903.
31. Nørholm MHH, Shulga YV, Aoki S, Epand RM, von Heijne G. Flanking residues help determine whether a hydrophobic segment adopts a monotopic or bitopic topology in the endoplasmic reticulum membrane. J. Biol. Chem. 2011; 286:25284–25290. [PubMed: 21606504]
32. Soldin, SJ.; Brugnara, C.; Wong, EC., editors. Pediatric Reference Intervals. AACC Press; Washington, DC: 2005.
33. Sellier-Leclerc A-L, et al. Differential impact of complement mutations on clinical characteristics in atypical hemolytic uremic syndrome. J. Am. Soc. Nephrol. 2007; 18:2392–2400. [PubMed: 17599974]
34. Frémeaux-Bacchi V, et al. Genetics and outcome of atypical hemolytic uremic syndrome: a nationwide French series comparing children and adults. Clin. J. Am. Soc. Nephrol. 2013 doi: 10.2215/CJN.04760512.
35. Roumenina LT, et al. Alternative complement pathway assessment in patients with atypical HUS. J. Immunol. Methods. 2011; 365:8–26. [PubMed: 21215749]
36. Boyden LM, et al. Mutations in kelch-like 3 and cullin 3 cause hypertension and electrolyte abnormalities. Nature. 2012; 482:98–102. [PubMed: 22266938]
37. Li H, et al. The Sequence Alignment/Map format and SAMtools. Bioinformatics. 2009; 25:2078–2079. [PubMed: 19505943]
38. Barrett JC, Fry B, Maller J, Daly MJ. Haploview: analysis and visualization of LD and haplotype maps. Bioinformatics. 2005; 21:263–265. [PubMed: 15297300]
39. Purcell S, et al. PLINK: a tool set for whole-genome association and population-based linkage analyses. Am. J. Hum. Genet. 2007; 81:559–575. [PubMed: 17701901]
40. Price AL, et al. Principal components analysis corrects for stratification in genome-wide association studies. Nat. Genet. 2006; 38:904–909. [PubMed: 16862161]
41. Reeve JP, Rannala B. DMLE+: Bayesian linkage disequilibrium gene mapping. Bioinformatics. 2002; 18:894–895. [PubMed: 12075030]
42. Genin E, Tullio-Pelet A, Begeot F, Lyonnet S, Abel L. Estimating the age of rare disease mutations: the example of Triple-A syndrome. J. Med. Genet. 2004; 41:445–449. [PubMed: 15173230]

43. Gudbjartsson DF, Jonasson K, Frigge ML, Kong A. Allegro, a new computer program for multipoint linkage analysis. Nat. Genet. 2000; 25:12–13. [PubMed: 10802644]

44. Thiele H, Nürnberg P. HaploPainter: a tool for drawing pedigrees with complex haplotypes. Bioinformatics. 2005; 21:1730–1732. [PubMed: 15377505]

45. Tang WH, et al. Glucose and collagen regulate human platelet activity through aldose reductase induction of thromboxane. J. Clin. Invest. 2011; 121:4462–4476. [PubMed: 22005299]

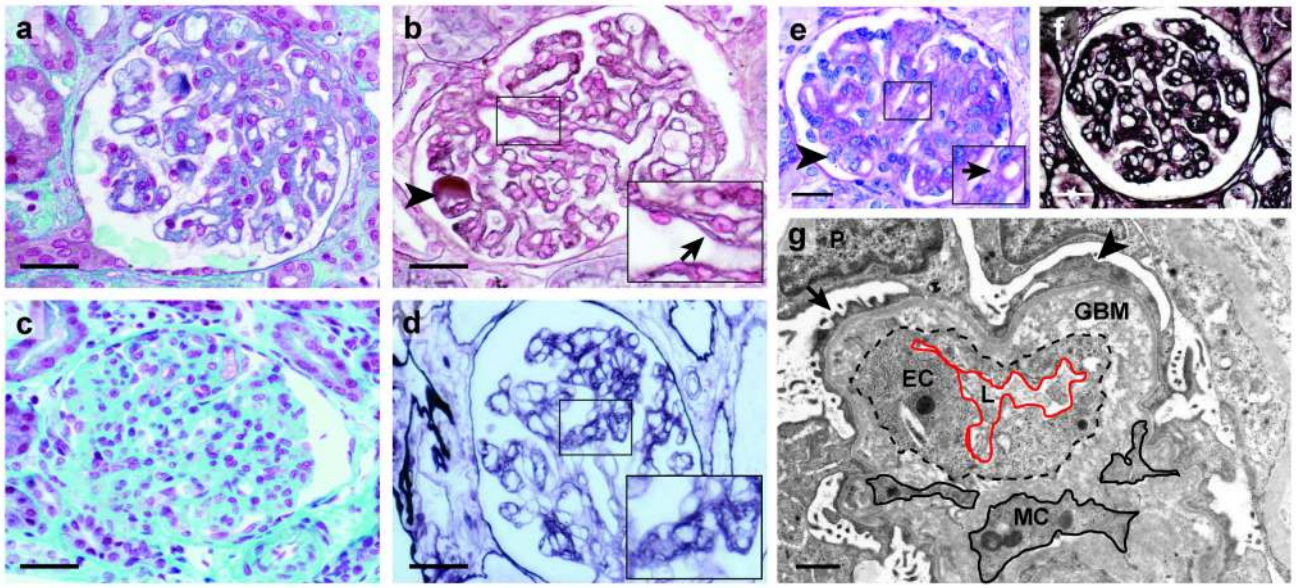

Figure 1.

Kidney biopsies of patients with *DGKE* mutations show histological features of chronic thrombotic microangiopathy. These include glomerular hypercellularity and split glomerular basement membranes (GBM) by light microscopy, and endothelial cells (EC) swelling and GBM internal lamina rara widening without electron-dense deposits on electron microscopy. (**a-b**) Renal biopsy of subject 1-3 at age 2. (**a**) Image shows reduced glomerular capillary lumen, increased mesangial matrix with mesangial hypercellularity, and patchy interstitial fibrosis (Masson's trichrome). (**b**) Glomerulus shows split GBM with debris accumulation in subendothelial space, and a dilated capillary filled with fibrinous material (arrowhead), consistent with a small thrombus (Jones' stain). (**c-d**) Renal biopsy of subject 1-3 at age 9, showing progression of renal damage. (**c**) Image shows bloodless, markedly lobular glomerulus with extensive fibrosis (Masson's trichrome). (**d**) Image shows enhanced global GBM splitting (inset; Jones' stain). (**e-g**) Renal biopsy of subject 4-1 at age 1. (**e**) Image shows global thickening of capillary walls, split GBM (arrow in inset), focal increase in mesangial matrix, and a prominent podocyte nucleus (arrowhead; Periodic acid-Schiff). (**f**) Image illustrates split and thickened GBM (Jones' stain). (**g**) Electron micrograph shows a narrow capillary lumen (L, red line) caused by GBM inner lamina rara expansion (devoid of electron-dense deposits) and hypertrophy of EC (black dotted line). There are also podocytes (P) with normal (arrow) or effaced (arrowhead) foot processes. Mesangial cell (MC; black line) processes are observed between EC and GBM, consistent with MC interposition (Lead citrate and uranyl acetate). Scale bars, 50 μm for **a-f**, 1 μm for **g**.

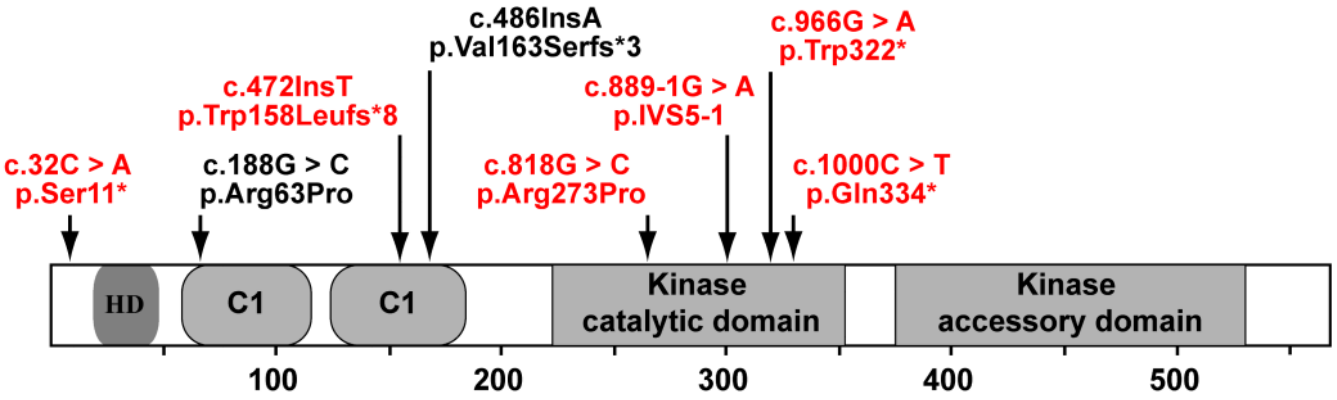

Figure 2.

DGKE mutations in aHUS. Schematic of DGKE domains is shown. C1 domains bind diacylglycerol; there is evidence that the hydrophobic domain (HD) is a transmembrane domain[31]. The locations and consequences of recessive mutations found in patients from 9 unrelated kindreds with aHUS are shown. Mutations that are homozygous in one or more families are shown in red; the remainders are found as compound heterozygotes. Genotypes in each affected patient are shown in Table 1. Pedigrees and sequence chromatograms are shown in Supplementary Fig. 1.

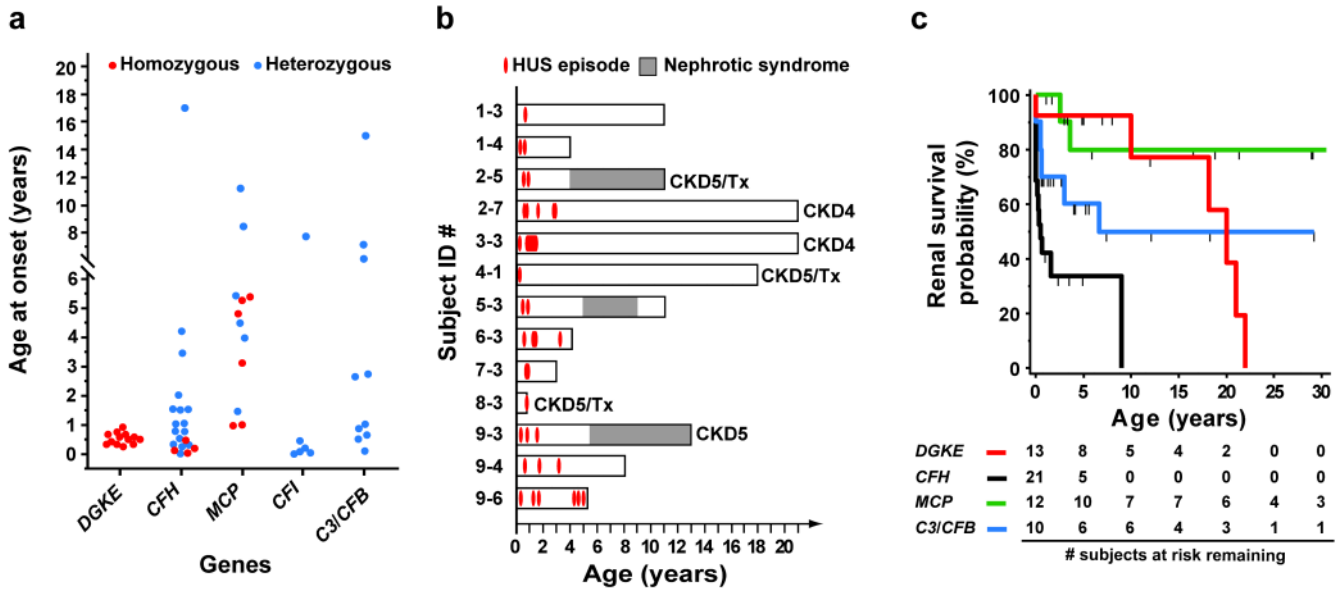

Figure 3.

Clinical course of aHUS due to *DGKE* mutation. (**a**) The age at onset of the first HUS episode is shown for all pediatric patients from the French aHUS cohort for whom mutations have been identified. Patients with DGKE mutation are notable for uniformly early diagnosis. (**b**) The ages of acute episodes HUS (red ovals) are shown. Gray shading denotes ages at which nephrotic syndrome was present. Subjects who developed chronic kidney disease stage 4 or 5 or were transplanted are labeled as “CKD4”, “CKD5”, or “Tx”, respectively. Subject 5-3 has had no detectable proteinuria after age 9. (**c**) Kaplan-Meier curve for renal survival, defined as CKD stage 3 or less, from patients with specific mutations causing aHUS from the French cohort. The table below the graph describes the number of patients who remain at risk for CKD stage 4 or 5 at each 5-year interval. The black vertical line located under each curve represent patients that are censored due to age. Curves for the most commonly mutated genes (*CFH*, *MCP*, *C3* and *CFB*) are compared to *DGKE*. P-values: *DGKE* vs. *CFH*, $P < 0.001$; *DGKE* vs. *MCP*, $P = 0.047$, *DGKE* vs. *C3*/*CFB*, $P > 0.05$. *CFH*, complement factor H; *CFB*, complement factors B; *C3*, complement component 3; *MCP*, membrane cofactor protein.

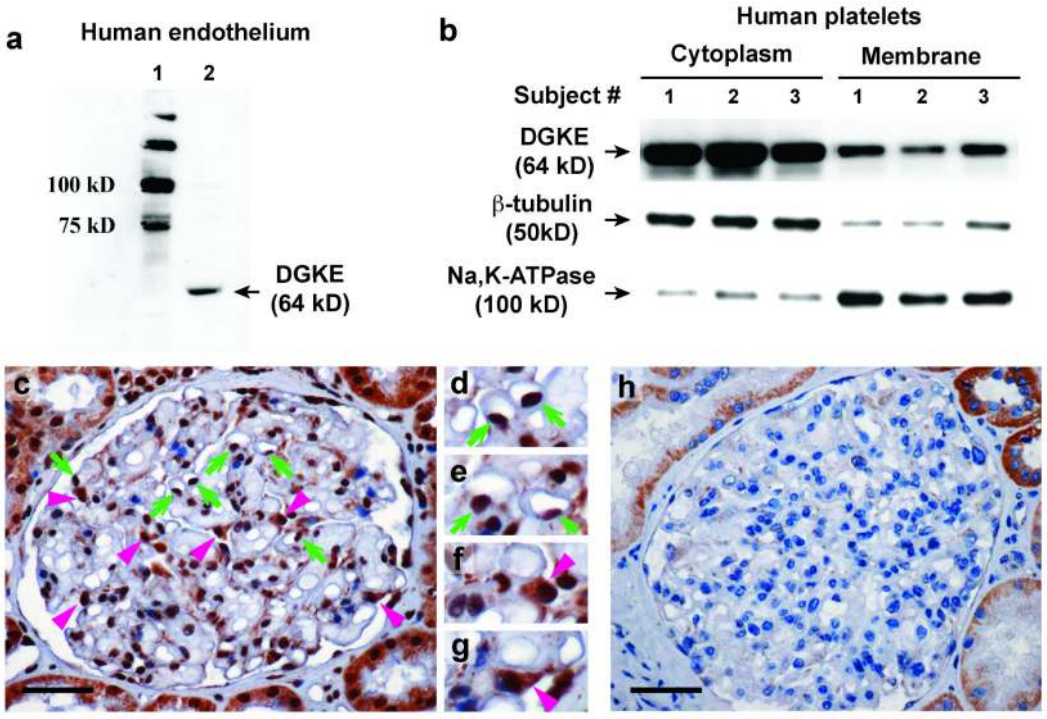

Figure 4.

DGKE protein is expressed in endothelium, platelets and podocytes. (**a**) Western blot of total protein extracted from human umbilical vein endothelial cells (HUVEC) probed with anti-DGKE antibody identifies a protein the expected size of DGKE (lane 2). Lane 1: molecular weight markers. (**b**) DGKE protein is present in both the cytoplasmic and membrane fractions of unstimulated platelets extracted from healthy human control subjects. Protein was extracted from cytoplasmic and membrane fractions of platelets and 50 μg of protein per lane was analyzed by Western blotting; the antibodies used are directed against DGKE, β-tubulin and the Na,K-ATPase. Similar results were found in analysis of platelets of wild type C57/BL6 adult mice, and relative DGKE levels do not change with age (Supplementary Fig. 6). (**c**) DGKE is expressed in glomerular podocytes and endothelial cells in normal human kidney. Kidney sections were stained with anti-DGKE antibodies exposed to immunoperoxidase-DAB (5 minutes) as described in Methods. Examples of DGKE-positive endothelial cells and podocytes are indicated by green arrows and pink arrowheads, respectively (DAB hematoxylin). **(d)** Higher magnification of endothelial cell from panel **(c). (e)** Higher magnification of endothelial cell from panel **(c)**. **(f)** Higher magnification of podocyte from panel **(c). (g)** Higher magnification of podocyte from panel (c). (**h**) Staining of kidney biopsy from patient 2-7 with anti-DGKE in parallel with section in panel (**c**) shows no evidence of glomerular DGKE expression. Controls for anti-DGKE staining, co-staining with anti-WT1 and staining with another anti-DGKE antibody are shown in Supplementary Fig. 7 and 8. Scale bars, 50 μm. DAB, 3,3′-diaminobenzidine.

Table 1

Demographic, laboratory and clinical characteristics for patients with *DGKE* nephropathy[a]

Subject ID	Age at Dx (yr), Gender	Hgb nadir nl>10.3 g/dL)	Evidence of MA[b]	PLT (nl<220 x10^9/L)	Cr (nl<0.2 mg/dL)	Dialysis at onset	Dx of first renal Bx (age, yr)	*DGKE* mutation 1	*DGKE* mutation 2
1-3	0.7, M	7.2	Yes	50	2.84	Yes	cTMA (2)	p.Trp322*	p.Trp322*
1-4	0.3, F	5.7	Yes	36	1.89	Yes	nd	p.Trp322*	p.Trp322*
2-5[c]	0.6, F	7.3	Yes	35	5.32	No	cTMA (1)	p.Arg63Pro	p.Val163Serfs*3
2-7[c]	0.3, F	6.8	Yes	168	1.35	No	cTMA (1.5)	p.Arg63Pro	p.Val163Serfs*3
3-3[c]	0.5, F	8.4	Yes	132	0.62	No	cTMA (0.7)	p.Trp322*	p.Ser11*
4-1[c]	0.3, F	3.7	Yes	390	8.51	Yes	cTMA (1)	p.Trp322*	p.Trp322*
5-3[c]	0.6, M	7.1	Yes	88	5.09	Yes	cTMA (1)	p.Trp322*	p.Trp158Leufs*8
6-3	0.5, F	9.0	Yes	99	2.52	Yes	cTMA (1)	p.Gln334*	p.Gln334*
7-3	0.9, M	4.9	Yes	125	6.79	Yes	cTMA (2)	p.IVS5-1	p.IVS5-1
8-3	0.7, M	5.0	Yes	214	7.19	Yes	cTMA (1[e])	p.Trp322*	p.Trp322*
9-3	0.3, M	6.4	Yes	33	4.21	Yes	cTMA (7)	p.Arg273Pro	p.Arg273Pro
9-4	0.8, M	8.2	nd	57	0.6	No	nd	p.Arg273Pro	p.Arg273Pro
9-6	0.3, F	7.3	Yes	32	2.21	Yes	nd	p.Arg273Pro	p.Arg273Pro

Bx, biopsy; Cr, creatinine; Dx, diagnosis; cTMA, chronic thrombotic microangiopathy; Hgb, hemoglobin; MA, microangiopathy; nd, not done; nl, normal; PLT, platelet count.

[a] Reference values for infants <1 year of age[32].

[b] Microangiopathy diagnosed by high lactate dehydrogenase, low haptoglobin and/or schistocytes on blood smear (details in Supplementary Table 2).

[c] Kindreds previously reported[33].

[d] Patient had many normal platelet counts with acute aHUS.

[e] Global renal cortical ischemia and malignant nephroangiosclerosis noted in both kidneys.